Report

Current Biology

Innate Predator Odor Aversion Driven by Parallel Olfactory Subsystems that Converge in the Ventromedial Hypothalamus

Highlights

- Individual predator kairomones activate distinct olfactory subsystems
- These diverse subsystems can each mediate innate aversion to select kairomones
- Kairomone information converges in medial amygdala and ventromedial hypothalamus

Authors

Anabel Pérez-Gómez, Katherin Bleymehl, ..., Frank Zufall, Pablo Chamero

Correspondence

frank.zufall@uks.eu

In Brief

Pérez-Gómez et al. reveal the parallel roles of three olfactory subsystems of the murine nose in the control of predator-odor-evoked avoidance behavior. The authors dissect the function of these subsystems in kairomone aversion and map their converging brain targets in the medial amygdala and ventromedial hypothalamus.

Pérez-Gómez et al., 2015, Current Biology *25*, 1340–1346
May 18, 2015 ©2015 Elsevier Ltd All rights reserved
http://dx.doi.org/10.1016/j.cub.2015.03.026

CellPress

Current Biology
Report

Innate Predator Odor Aversion Driven by Parallel Olfactory Subsystems that Converge in the Ventromedial Hypothalamus

Anabel Pérez-Gómez,[1] Katherin Bleymehl,[1] Benjamin Stein,[1] Martina Pyrski,[1] Lutz Birnbaumer,[2,4] Steven D. Munger,[3] Trese Leinders-Zufall,[1,5] Frank Zufall,[1,5,*] and Pablo Chamero[1,5]
[1]Department of Physiology and Center for Integrative Physiology and Molecular Medicine, University of Saarland School of Medicine, 66421 Homburg, Germany
[2]Laboratory of Neurobiology, National Institute of Environmental Health Sciences, Research Triangle Park, NC 27709, USA
[3]Department of Pharmacology and Therapeutics, Department of Medicine, Division of Endocrinology, Diabetes and Metabolism, and Center for Smell and Taste, University of Florida, Gainesville, FL 32610, USA
[4]Present address: Instituto de Investigaciones Biotecnológicas, Universidad Nacional de San Martín, San Martín, Provincia de Buenos Aires (1650), Argentina
[5]Co-senior author
*Correspondence: frank.zufall@uks.eu
http://dx.doi.org/10.1016/j.cub.2015.03.026

SUMMARY

The existence of innate predator aversion evoked by predator-derived chemostimuli called kairomones offers a strong selective advantage for potential prey animals. However, it is unclear how chemically diverse kairomones can elicit similar avoidance behaviors. Using a combination of behavioral analyses and single-cell Ca^{2+} imaging in wild-type and gene-targeted mice, we show that innate predator-evoked avoidance is driven by parallel, non-redundant processing of volatile and nonvolatile kairomones through the activation of multiple olfactory subsystems including the Grueneberg ganglion, the vomeronasal organ, and chemosensory neurons within the main olfactory epithelium. Perturbation of chemosensory responses in specific subsystems through disruption of genes encoding key sensory transduction proteins (*Cnga3*, *Gnao1*) or by surgical axotomy abolished avoidance behaviors and/or cellular Ca^{2+} responses to different predator odors. Stimulation of these different subsystems resulted in the activation of widely distributed target regions in the olfactory bulb, as assessed by c-Fos expression. However, in each case, this c-Fos increase was observed within the same subnuclei of the medial amygdala and ventromedial hypothalamus, regions implicated in fear, anxiety, and defensive behaviors. Thus, the mammalian olfactory system has evolved multiple, parallel mechanisms for kairomone detection that converge in the brain to facilitate a common behavioral response. Our findings provide significant insights into the genetic substrates and circuit logic of predator-driven innate aversion and may serve as a valuable model for studying instinctive fear [1] and human emotional and panic disorders [2, 3].

RESULTS AND DISCUSSION

The mammalian olfactory system is composed of a variety of subsystems that rely on distinct sensory neuron subpopulations for chemodetection [4–7]. Three of these sensory neuron groups—the vomeronasal organ (VNO) [8–10], the Grueneberg ganglion (GG) [11], and subsets of sensory neurons within the main olfactory epithelium (MOE) that express trace amine-associated receptors (Taars) [7, 12, 13]—have been implicated in predator odor aversion through their detection of kairomones, which are semiochemicals released by one species that benefit a member of another species [14]. To better understand how instinctive behaviors are initiated and controlled by these subsystems, how odor-driven activity from each subsystem is represented and integrated by higher structures in the CNS, and what functional contributions each subsystem makes to social behaviors, we focused on a functional dissection of innate kairomone aversion in mice.

Defensive Behaviors Evoked by Different Predator Odors

Naive wild-type male mice (C57BL/6, denoted hereafter as B6) were presented a range of predator-derived odors (Figure 1A), and behavior was monitored automatically (see Supplemental Experimental Procedures). We systematically compared several predator odors whose nasal detection has been associated with distinct olfactory substructures: TMT (2,5-dihydro-2,4,5- trimethylthiazole), which is present in fox feces and activates both the MOE and GG [11, 15]; PEA (β-phenylethylamine), which is found in carnivore urine and activates Taar4 neurons of the MOE [12, 13]; cat fur odor (CFO), which activates the VNO [9, 10]; and 2-PT (2-propylthietane), a GG activator from the stoat anal gland [11] (Figure 1B). Objects impregnated with each stimulus were presented in single trials, and behavior was quantified as time spent in the vicinity of the stimulus (Figure 1C), average location in the test cage (Figures 1D and 1E), and accumulated distance walked (Figure 1F). All four predator odors elicited robust avoidance in B6 mice (Figures 1C–1G). Additionally, some stimuli also

 ©2015 Elsevier Ltd All rights reserved

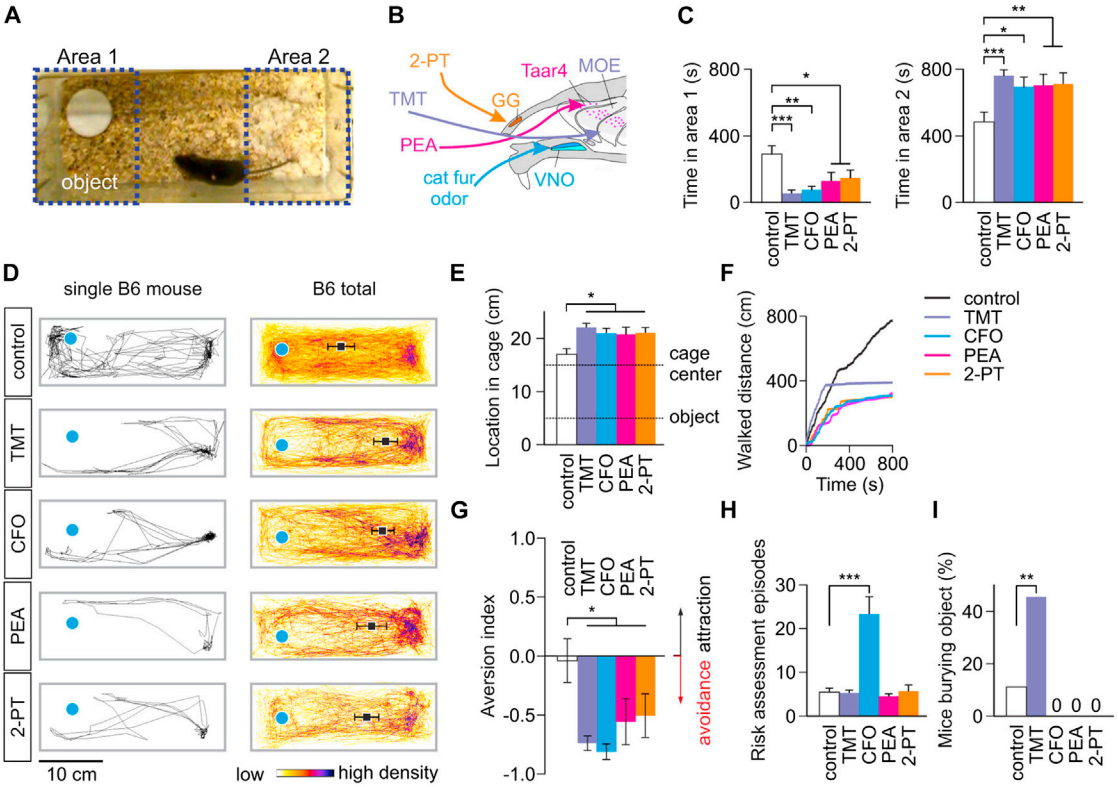

Figure 1. Comparing Innate Defensive Behaviors Driven by Different Predator Odors

(A) Example of a video frame demonstrating the behavioral assay, in which a male mouse is exposed to a cotton pad impregnated with a particular predator odor (object). Time spent in area 1 or 2 was quantified.

(B) Schematic showing proposed olfactory subsystem specificity of the predator odors tested. 2-PT, 2-propylthietane; Taar4, trace amine-associated receptor 4-expressing neurons; MOE, main olfactory epithelium; TMT, 2,5-dihydro-2,4,5-trimethylthiazole; GG, Grueneberg ganglion; PEA, β-phenylethylamine; VNO, vomeronasal organ.

(C) Average time spent by B6 mice in each of the opposing cage areas as depicted in (A). Object was placed in area 1 (n = 13–24 B6 mice for each odor exposure). PBS served as neutral control. Area 1: ANOVA: $F_{4,77} = 4.73$; $p < 0.005$; LSD: *$p < 0.05$; **$p < 0.01$; ***$p < 0.001$; area 2: ANOVA: $F_{4,77} = 4.15$; $p < 0.005$; LSD: *$p < 0.05$; **$p < 0.01$; ***$p < 0.001$.

(D) Trajectory plots of the position of a representative B6 mouse (left panels, single B6 mouse) and corresponding heatmap graphs of all tested mice (right panels, B6 total) in response to 15 min exposures to predator odor (blue circle indicates object position). The black squares in the heatmap graphs represent the average position of the animals in the cage.

(E) Average position of B6 mice in the test cage during the 15 min assay. Cages were 30 cm long, and objects were placed approximately 5 cm from the edge of the cage. ANOVA: $F_{4,77} = 4.27$; $p < 0.005$; LSD: *$p < 0.05$.

(F) Average accumulated distance walked during a 15 min exposure to different predator odors (n = 13–24 B6 mice for each predator odor).

(G) Average response to a given stimulus, as quantified by the aversion index. For each stimulus and mouse, we defined a performance index (see Supplemental Experimental Procedures) wherein avoidance is indicated by a negative value and attraction by a positive one. ANOVA: $F_{4,74} = 4.24$; LSD: *$p < 0.05$.

(H) Number of risk assessment episodes displayed during exposure to different predator odors. CFO, but not TMT, PEA, or 2-PT, evoked a significant increase in the number of risk assessment episodes. ANOVA: $F_{4,65} = 18.21$; LSD: ***$p < 0.001$.

(I) Percentage of animals burying the object in the cage bedding. TMT, but not CFO, PEA, or 2-PT, evoked defensive burying behavior. ANOVA: $F_{4,65} = 5.93$; LSD: **$p < 0.005$ (n = 11–18).

Results are presented as means ± SEM.

produced other types of defensive behaviors. For example, CFO but not TMT, PEA, or 2-PT induced an elevated number of risk-assessment episodes (Figure 1H), characterized by an investigative extended body posture [16]. TMT but not CFO, PEA, or 2-PT caused mice to bury the stimulus in the cage bedding (Figure 1I). Therefore, all four stimuli evoke a coherent behavioral output, innate predator odor aversion. Other forms of defensive behavior, such as risk assessment and object burying, are displayed only in response to select stimuli.

Kairomones Engage Gαo-Dependent and -Independent Pathways

To dissect the peripheral neural pathways necessary for innate predator odor aversion, we analyzed behavioral and cellular responses of mutant mice deficient for specific signal transduction components. We first used a mutant strain (cGαo$^{-/-}$ mice) in which the *Gnao1* gene (encoding the G protein Gαo) was conditionally deleted under the control of the *Omp* (olfactory marker protein) gene [17, 18]. Gαo is essential for sensory transduction in vomeronasal sensory neurons (VSNs) of the basal layer of the

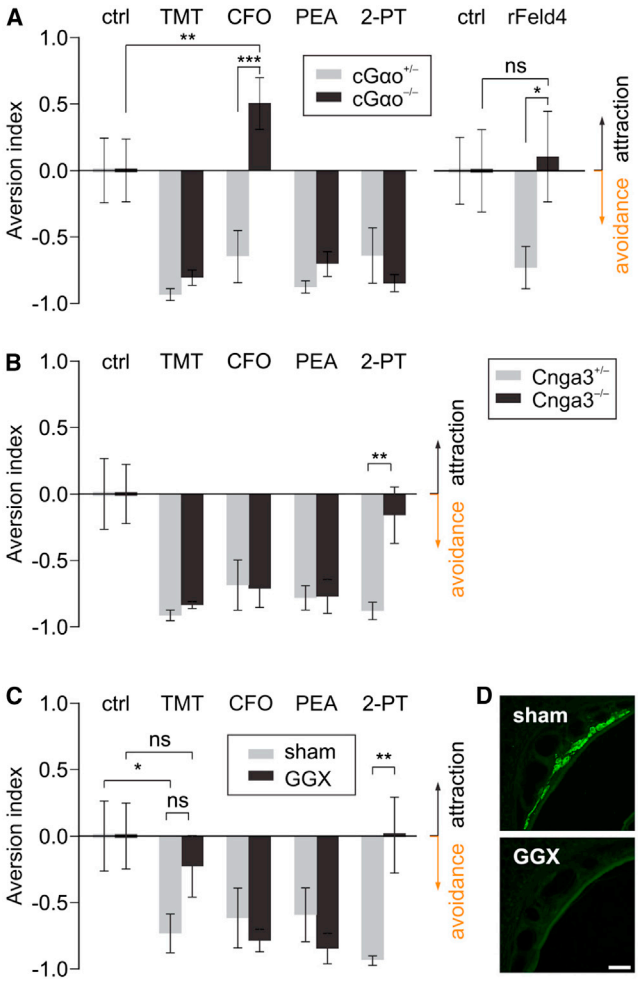

Figure 2. Genetic Dissection of Innate Aversion

(A) Aversion index of cGαo$^{-/-}$ (black) versus cGαo$^{+/-}$ (gray) mice exposed to control (ctrl), TMT, CFO, PEA, 2-PT, or rFeld4. The avoidance to CFO and rFeld4 depends on Gαo. ANOVA: $F_{1,100} = 5.29$; LSD: *$p < 0.05$, **$p < 0.01$, ***$p < 0.001$, ns (not significant), $p = 0.79$ (n = 6–21).

(B) Aversion index of *Cnga3*$^{-/-}$ versus *Cnga3*$^{+/-}$ mice exposed to the set of predator odors, demonstrating that avoidance to 2-PT requires Cnga3 whereas avoidance to TMT, CFO, or PEA does not. ANOVA: $F_{1,129} = 2.33$; LSD: **$p < 0.01$ (n = 13 mice per genotype).

(C) Aversion index for sham-operated and GG-axotomized (GGX) mice exposed to the set of predator odors. Two-way ANOVA: $F_{1,99} = 2.26$; LSD: *$p < 0.05$, **$p < 0.01$, ns (not significant), $p = 0.08$ (TMT sham versus TMT GGX), $p = 0.4$ (GGX control versus GGX TMT) (n = 10 mice per condition).

(D) OMP immunofluorescence performed on GG histological sections 4 weeks after axotomy (GGX; bottom) and in sham-operated animals (top). Green OMP fluorescence is detected in intact GGNs. Scale bar, 50 μm.

Results are presented as means ± SEM.

vomeronasal sensory epithelium [17], which detect nonvolatile peptides and major urinary proteins (MUPs) [19]. In behavioral studies, CFO avoidance was abolished in cGαo$^{-/-}$ mice (Figures 2A, S1G, and S1I), while CFO-induced risk assessment was significantly reduced compared to cGαo$^{+/-}$ controls (Figure S1H). By contrast, the avoidance evoked by TMT, PEA, and 2-PT in cGαo$^{-/-}$ mice was indistinguishable from controls (Figure 2A), indicating that these three stimuli engage Gαo-independent signal transduction mechanisms. Avoidance of the candidate kairomone protein Feld4, a MUP-like ortholog present in cat saliva that elicits avoidance behavior in mice in a Trpc2-dependent manner [10], was similarly abolished in cGαo$^{-/-}$ mice (Figures 2A and S1A–S1F). Ratiometric Ca^{2+} imaging of freshly dissociated VSNs [17, 20, 21] showed that both CFO and Feld4 (500 nM) activated ~2% of cells screened in either B6 or cGαo$^{+/-}$ controls (n = 8,000–12,000 cells; Figures S1J and S1K); a large fraction of cells activated by CFO (47%) were also activated by rFeld4 (Figures S1J and S1K). By contrast, VSNs from cGαo$^{-/-}$ mice revealed a drastic reduction ($p < 0.001$) in responses to rFeld4, comparable to background (control) activity levels and consistent with the idea that this protein is detected only by basal VSNs (Figures S1J and S1K). Interestingly, cGαo$^{-/-}$ mice also displayed some attraction to CFO (Figure 2A), indicating that they are not anosmic for this stimulus. This emergent behavior likely results from responses to attractive components of this complex stimulus that are unmasked once responses to aversive components are eliminated. Indeed, a fraction of Gαo$^{-/-}$ cells showed responses to CFO at levels ~50% of those seen in controls ($p < 0.001$), but there was no overlap between CFO-induced activity and background responses obtained with rFeld4 in Gαo$^{-/-}$ cells (data not shown). Additionally, cGαo$^{-/-}$ mice showed no attraction to Feld4 (Figure 2A). Therefore, CFO is detected by both Gαo-dependent and -independent vomeronasal transduction mechanisms, whereas rFeld4 detection depends solely on Gαo-dependent sensing. Despite a loss of sensory function in the basal VSNs, the VNO of cGαo$^{-/-}$ mice still retains the ability to detect at least some CFO components (e.g., by apical VSNs that do not require Gαo for transduction) even though this activity is not sufficient to drive innate avoidance behavior.

Cnga3 Null Mice Enable Dissection of Innate Kairomone Aversion by the Grueneberg Ganglion

We performed further experiments using OMP-GFP/Cnga3 mutant mice (*Cnga3*$^{-/-}$ or *Cnga3*$^{+/-}$ mice) [22]. These mice lack the cyclic nucleotide-gated (CNG) channel subunit Cnga3 [23–25] and express GFP in all OMP-expressing cells. Behavioral analyses in *Cnga3*$^{+/-}$ versus *Cnga3*$^{-/-}$ mice revealed that the avoidance to 2-PT was nearly eliminated in *Cnga3*$^{-/-}$ mice ($p < 0.01$), whereas the aversion evoked by TMT, CFO, and PEA remained normal (Figures 2B and S2A–S2C). Cnga3 is expressed both in the GG [26, 27] and in small subsets of sensory neurons in the MOE and the septal organ that also express the guanylyl cyclase GC-D (~0.1% of OSNs) [23, 28, 29]. Surgical axotomy of the GG (GGX; Figure 2D) eliminated the innate avoidance to 2-PT ($p < 0.01$), but not that to CFO or PEA (Figures 2C and S2D–S2F), indicating that 2-PT-evoked avoidance is driven solely by the GG. Although GGX mice showed a trend toward reduced aversion to TMT, this difference was not significant compared to controls (Figure 2C; least significant difference [LSD]: $p = 0.085$). Interestingly, GGX mice, but not *Cnga3*$^{-/-}$ mice, failed to bury objects impregnated with TMT (Figures S2C and S2F), indicating that TMT-evoked object burying is also driven by the GG. However, a functional Cnga3 channel was not required for this effect (Figure S2C). Time-resolved cellular analyses using ratiometric Ca^{2+} imaging on acute GG tissue slices obtained from OMP-GFP$^{+/-}$, *Cnga3*$^{+/-}$, and *Cnga3*$^{-/-}$

 ©2015 Elsevier Ltd All rights reserved

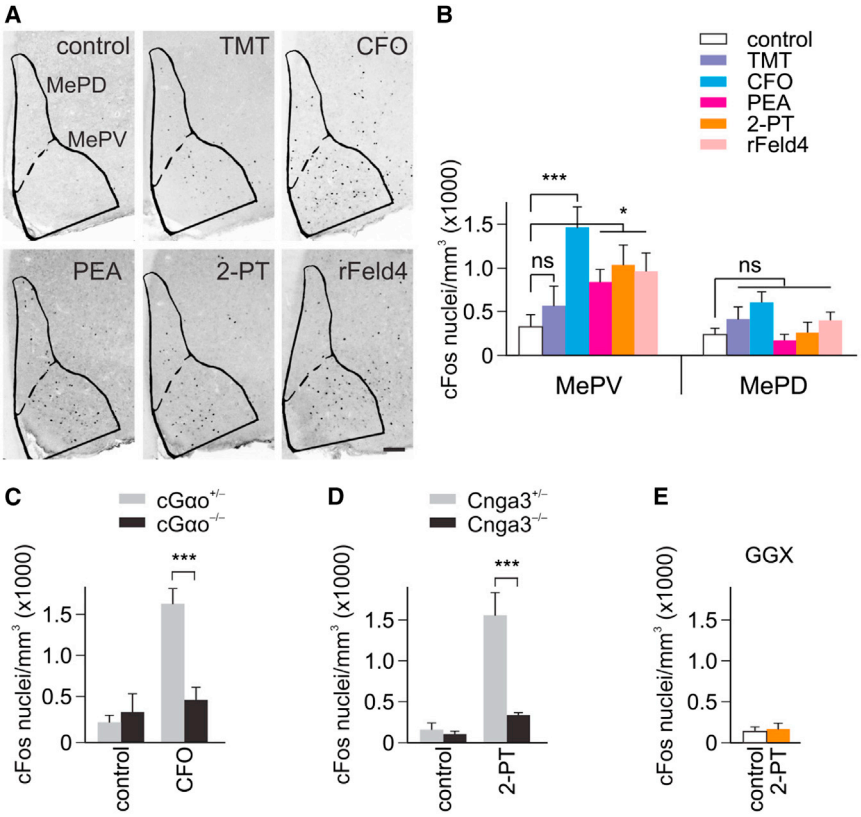

Figure 3. The Posteroventral Medial Amygdala Is Activated by Predator Signals Originating from the Grueneberg Ganglion, the VNO, and the Taar System

(A) Examples of c-Fos activation on coronal sections through MeA of B6 mice exposed to various predator odors. MePD, posterodorsal medial amygdala; MePV, posteroventral medial amygdala. c-Fos+ nuclei were counted blindly for each genotype or treatment. Images (bregma −1.46 mm) are displayed as color-inverted negative of original fluorescent black-and-white images. Scale bars, 100 μm.

(B) Quantification of c-Fos+ nuclei of B6 mice indicates that MePV, but not MePD, is activated by CFO, PEA, 2-PT, and rFeld4. The effect of TMT was not significantly different from control.

(C–E) Quantification of c-Fos+ nuclei in the MePV of cGαo$^{+/-}$ and cGαo$^{-/-}$ mice (C), *Cnga3*$^{+/-}$ and *Cnga3*$^{-/-}$ mice (D), and GGX mice (E). B6: ANOVA: $F_{5,36}$ = 3.39–4.64; cGαo: ANOVA: $F_{1,24}$ = 10.65; Cnga3: ANOVA: $F_{1,23}$ = 14.11; LSD: *p < 0.05, ***p < 0.001, ns (not significant). GGX: t test: p = 0.98. n = 5–8 mice per stimulus and genotype. Results are presented as means ± SEM.

mice [22] in response to chemostimulation supported this division (Figures S2G–S2K). We identified two major subpopulations of GG neurons (GGNs) in OMP-GFP$^{+/-}$ and *Cnga3*$^{+/-}$ mice: one (nearly 50% of the cells, type 1) that detects 2-PT but not TMT, and another (about 25% of the cells, type 2) that senses TMT but not 2-PT (Figures S2I and S2J). Importantly, whereas the responses of *Cnga3*$^{-/-}$ GGNs to 2-PT were nearly absent, those to TMT were similar to controls regardless of the parameter analyzed (e.g., number of responding cells or size of the Ca^{2+} responses) (Figures S2J and S2K). Therefore, Cnga3 is essential for chemosensory transduction in a subset of GGNs that detect the predator odor 2-PT, but not TMT, and these neurons are likely required for driving innate aversion to 2-PT. By contrast, GGN detection of TMT is largely independent of Cnga3.

Segregated Kairomone Representation in the Olfactory Bulb

Next, we mapped neural activation in the olfactory bulb following kairomone exposure using immunodetection of the immediate early gene c-Fos. In the accessory olfactory bulb (AOB), we observed a significant increase in the number of c-Fos+ nuclei in B6 mice exposed to either CFO or rFeld4, but not to TMT, 2-PT, or PEA (Figures S3A–S3C). Consistent with results from our Ca^{2+}-imaging experiments, CFO-evoked c-Fos was found in both the anterior and posterior AOB, whereas rFeld4 exposure activated only the posterior AOB (Figures S3A–S3C). In cGαo$^{-/-}$ mice, CFO-induced c-Fos was detected in the anterior but not posterior AOB (Figures S3D and S3E). Therefore, CFO induces activation of the AOB in both Gαo+ (posterior) and Gαi2+ (anterior) zones, but the activity of the Gαi2+ zone alone is not sufficient to drive innate avoidance behavior.

The necklace glomerulus region of the MOB is innervated by GGNs and GC-D+ OSNs, both of which express phosphodiesterase 2A (PDE2A) in their axons (Figure S3F). We observed a 6- to 8-fold increase in c-Fos+ cells in the immediate vicinity of PDE2A+ glomeruli of 2-PT- and TMT-exposed B6 mice (Figures S3G and S3H). 2-PT failed to induce any increase in c-Fos+ cells in *Cnga3*$^{-/-}$ mice, whereas TMT caused elevated (~7-fold) c-Fos activation in PDE2A+ glomeruli of both genotypes (Figures S3G and S3H). Similarly, the 2-PT-evoked increase in c-Fos+ cells was abolished whereas the TMT-evoked activity was only partially reduced in GGX mice (Figures S3G and S3H). Thus, 2-PT-evoked activity in the caudal OB depends entirely on GGN activation and requires a functional Cnga3 channel. TMT-evoked activation of the necklace system does not require Cnga3 and is only partially reduced by GG axotomy (Figure S3H), suggesting that these necklace glomeruli receive additional sensory input from TMT-detecting neurons located outside the GG, most likely in the MOE [15, 30]. Some OB glomeruli outside the necklace system are also activated by TMT ([31] and data not shown). Combined with the observation that PEA activates a distinct set of glomeruli in the dorsocaudal OB [32, 33], these findings demonstrate that the representation of predator odors in the OB remains highly distributed across the olfactory periphery and olfactory bulb.

Kairomone Information Converges in the Medial Amygdala and Ventromedial Hypothalamus

We next asked whether these pathways converge at higher levels of the CNS. Exposure of B6 mice to CFO (VNO), rFeld4

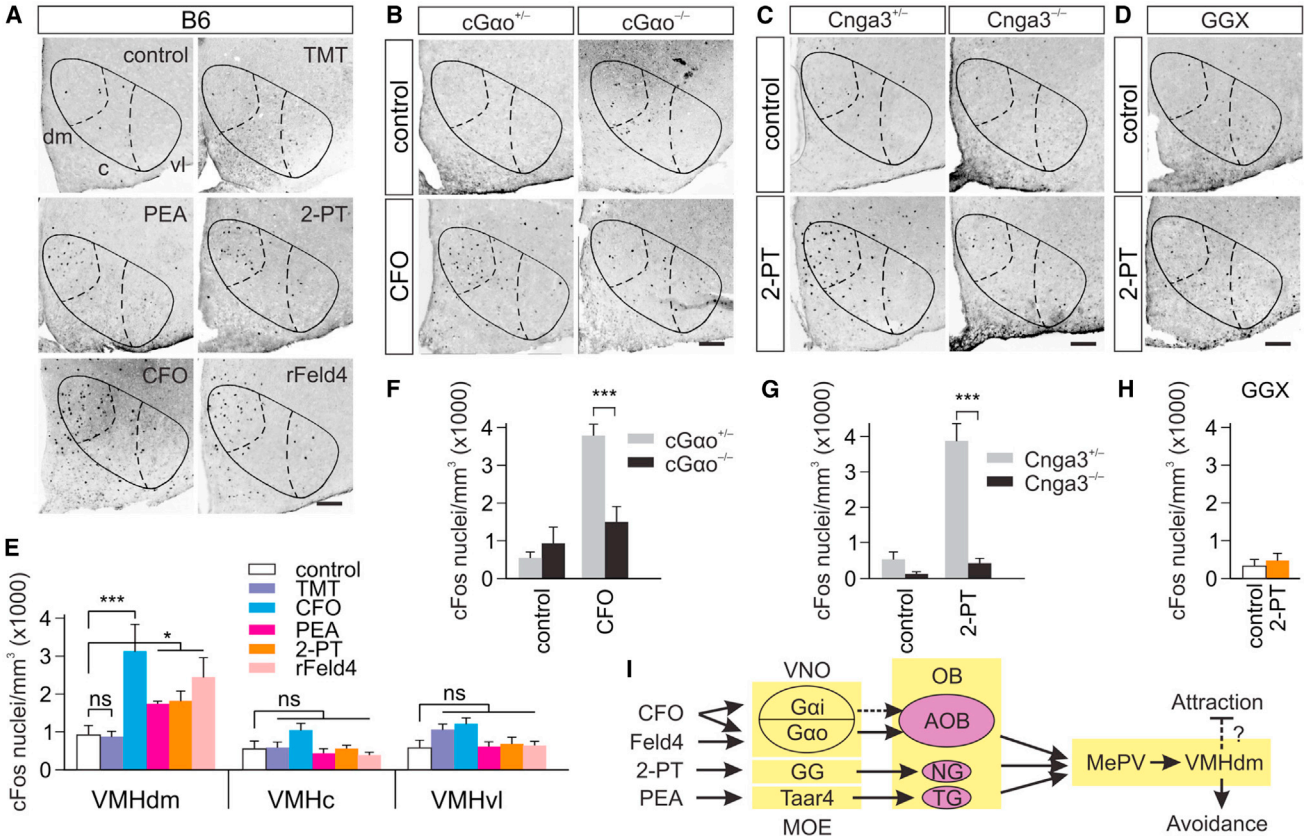

Figure 4. Cells in the VMH Dorsomedial Division Receive Sensory Input from Parallel Olfactory Subsystems Driving Innate Predator Odor Avoidance

(A–D) Examples of c-Fos activity in sections through the VMH of B6 (A), cGαo$^{-/-}$ (B), *Cnga3*$^{-/-}$ (C), and GGX (D) mice exposed to predator odors. Images (bregma −1.46 mm) are displayed as color-inverted negative of original fluorescent black-and-white images. dm, dorsomedial VMH; c, central VMH; vl, ventrolateral VMH. Scale bars, 100 μm.

(E) Quantification of c-Fos+ nuclei in the three VMH subdivisions indicates that VMHdm is activated by CFO, PEA, 2-PT, and rFeld4, but not by TMT. ANOVA: $F_{5,34}$ = 2.63–7.29.

(F–H) Quantification of c-Fos+ nuclei in VMHdm of cGαo$^{+/-}$ and cGαo$^{-/-}$ mice (F), *Cnga3*$^{+/-}$ and *Cnga3*$^{-/-}$ mice (G), and GGX mice (H). cGαo: ANOVA: $F_{1,21}$ = 15.72; Cnga3: ANOVA: $F_{3,23}$ = 31.7; LSD: *$p < 0.05$, ***$p < 0.001$, ns (not significant). GGX: t test: $p = 0.98$. n = 5–8 mice per stimulus and genotype.

(I) Schematic summarizing the results. In the context of innate predator odor avoidance, olfactory inputs from three different olfactory subsystems (VNO, GG, Taar system) are processed by separate, parallel neural pathways that provide converging sensory input to MePV and VMHdm. NG, necklace glomeruli; TG, Taar glomeruli.

Results are presented as means ± SEM.

(VNO), PEA (MOE), and 2-PT (GG) induced a 2- to 5-fold increase in the number of c-Fos+ cells in the medial amygdala (MeA) posteroventral division (MePV), but not in the posterodorsal MeA (MePD) (Figures 3A and 3B). These results suggest that this predator odor information must ultimately all target the MePV (see also [9]). By contrast, TMT failed to induce any significant increase in c-Fos in the MeA (Figures 3A and 3B; $p = 0.322$), consistent with previous mapping of TMT-dependent neuronal activation [31, 34, 35].

Our c-Fos mapping also revealed robust activation in response to PEA, 2-PT, CFO, and rFeld4 in a major MePV target region, the dorsomedial subdivision of the ventromedial hypothalamus (VMHdm) [36] (Figures 4A and 4E); the central (VMHc) and ventrolateral (VMHvl) aspects of the VMH lacked activation by any of these cues. CFO failed to elicit any increase in c-Fos+ cells in either the MeA (Figures 3C and S4A) or VMH (Figures 4B and 4F) of cGαo$^{-/-}$ mice. Similarly, the c-Fos increase to 2-PT was eliminated in the MeA (Figures 3D, 3E, S4B, and S4C) and VMH (Figures 4C, 4D, 4G, and 4H) of both *Cnga3*$^{-/-}$ and GGX mice. Thus, the activity we observe in MeA and VMH in response to CFO and 2-PT requires intact function of Gαo in basal VSNs and of Cnga3 in the GG, respectively. Consistent with the results in MeA, TMT did not induce a significant increase ($p = 0.921$) in c-Fos+ cells in any of the VMH regions (Figures 4A and 4E).

Conclusions

Our results indicate that the representation of diverse predator odors—initially widely distributed across the olfactory system—eventually becomes highly organized and spatially confined to specific subregions of the MeA and VMH (Figure 4I). In particular, our observations indicate a central role of VMHdm in the control of innate kairomone aversion. Our results are consistent with studies implicating the MePV in the control of fear and anxiety

 ©2015 Elsevier Ltd All rights reserved

responses [37–39] and the VMH in defensive, escape, avoidance, and panic-like behaviors in rodents [36, 40–47] and panic attacks in humans [3]. We conclude that the coding strategies underlying kairomone-mediated aversive behavior include (1) the involvement of multiple, distinct olfactory subsystems; (2) the parallel and relatively independent function of each subsystem in triggering innate avoidance in a non-redundant manner; and (3) the generation of converging sensory inputs by these olfactory subsystems to the same higher-order subnuclei of the CNS. An obvious advantage of these coding strategies in kairomone-mediated avoidance is that an animal receiving these signals would increase its chance of survival by enhancing receptor space to maximize the probability that a life-threatening predator is detected in a timely manner.

SUPPLEMENTAL INFORMATION

Supplemental Information includes four figures and Supplemental Experimental Procedures and can be found with this article online at http://dx.doi.org/10.1016/j.cub.2015.03.026.

AUTHOR CONTRIBUTIONS

A.P.-G., T.L.-Z., F.Z., and P.C. designed and initiated the study. A.P.-G. performed all behavioral experiments. B.S. and K.B. performed Ca^{2+} imaging in VSNs and GGNs. A.P.-G. and M.P. performed immunohistochemistry. M.P. performed all lesions. A.P.-G., K.B., B.S., M.P, T.L.-Z., and P.C. analyzed data. L.B. provided mouse models. S.D.M., T.L.-Z., F.Z., and P.C. wrote the manuscript with editing input from all authors.

ACKNOWLEDGMENTS

All animal care and experimental procedures were performed in accordance with guidelines established by the animal welfare committee of the University of Saarland. We thank Peter Mombaerts for supplying OMP-GFP and OMP-Cre mice, Martin Biel for providing Cnga3 null mice, and Lisa Stowers for the gift of the Feld4 plasmid. This work was supported by Deutsche Forschungsgemeinschaft grants CH 920/2-1 (P.C.), Sonderforschungsbereich 894 projects A16 (T.L.-Z.) and A17 (F.Z.), and International Graduate School GK 1326 (K.B.); National Institute on Deafness and Other Communication Disorders grant DC005633 (S.D.M. and F.Z.); a University of Saarland HOMFORexzellent grant (P.C.); the Intramural Research Program of the NIH to L.B. (project Z01 ES-101643); and the Volkswagen Foundation (T.L.-Z.). T.L.-Z. is also a Lichtenberg Professor of the Volkswagen Foundation.

Received: February 16, 2015
Revised: March 16, 2015
Accepted: March 17, 2015
Published: April 30, 2015

REFERENCES

1. Staples, L.G. (2010). Predator odor avoidance as a rodent model of anxiety: learning-mediated consequences beyond the initial exposure. Neurobiol. Learn. Mem. *94*, 435–445.
2. Blanchard, D.C., Griebel, G., and Blanchard, R.J. (2001). Mouse defensive behaviors: pharmacological and behavioral assays for anxiety and panic. Neurosci. Biobehav. Rev. *25*, 205–218.
3. Wilent, W.B., Oh, M.Y., Buetefisch, C.M., Bailes, J.E., Cantella, D., Angle, C., and Whiting, D.M. (2010). Induction of panic attack by stimulation of the ventromedial hypothalamus. J. Neurosurg. *112*, 1295–1298.
4. Ma, M. (2007). Encoding olfactory signals via multiple chemosensory systems. Crit. Rev. Biochem. Mol. Biol. *42*, 463–480.
5. Munger, S.D., Leinders-Zufall, T., and Zufall, F. (2009). Subsystem organization of the mammalian sense of smell. Annu. Rev. Physiol. *71*, 115–140.
6. Omura, M., and Mombaerts, P. (2014). Trpc2-expressing sensory neurons in the main olfactory epithelium of the mouse. Cell Rep. *8*, 583–595.
7. Liberles, S.D. (2015). Trace amine-associated receptors: ligands, neural circuits, and behaviors. Curr. Opin. Neurobiol. *34C*, 1–7.
8. McGregor, I.S., Hargreaves, G.A., Apfelbach, R., and Hunt, G.E. (2004). Neural correlates of cat odor-induced anxiety in rats: region-specific effects of the benzodiazepine midazolam. J. Neurosci. *24*, 4134–4144.
9. Samuelsen, C.L., and Meredith, M. (2009). The vomeronasal organ is required for the male mouse medial amygdala response to chemical-communication signals, as assessed by immediate early gene expression. Neuroscience *164*, 1468–1476.
10. Papes, F., Logan, D.W., and Stowers, L. (2010). The vomeronasal organ mediates interspecies defensive behaviors through detection of protein pheromone homologs. Cell *141*, 692–703.
11. Brechbühl, J., Moine, F., Klaey, M., Nenniger-Tosato, M., Hurni, N., Sporkert, F., Giroud, C., and Broillet, M.C. (2013). Mouse alarm pheromone shares structural similarity with predator scents. Proc. Natl. Acad. Sci. USA *110*, 4762–4767.
12. Ferrero, D.M., Lemon, J.K., Fluegge, D., Pashkovski, S.L., Korzan, W.J., Datta, S.R., Spehr, M., Fendt, M., and Liberles, S.D. (2011). Detection and avoidance of a carnivore odor by prey. Proc. Natl. Acad. Sci. USA *108*, 11235–11240.
13. Dewan, A., Pacifico, R., Zhan, R., Rinberg, D., and Bozza, T. (2013). Non-redundant coding of aversive odours in the main olfactory pathway. Nature *497*, 486–489.
14. Wyatt, T.D. (2014). Pheromones and Animal Behavior, Second Edition. (Cambridge Unversity Press).
15. Kobayakawa, K., Kobayakawa, R., Matsumoto, H., Oka, Y., Imai, T., Ikawa, M., Okabe, M., Ikeda, T., Itohara, S., Kikusui, T., *et al*. (2007). Innate versus learned odour processing in the mouse olfactory bulb. Nature *450*, 503–508.
16. Blanchard, R.J., Blanchard, D.C., Rodgers, J., and Weiss, S.M. (1990). The characterization and modelling of antipredator defensive behavior. Neurosci. Biobehav. Rev. *14*, 463–472.
17. Chamero, P., Katsoulidou, V., Hendrix, P., Bufe, B., Roberts, R., Matsunami, H., Abramowitz, J., Birnbaumer, L., Zufall, F., and Leinders-Zufall, T. (2011). G protein G(α)o is essential for vomeronasal function and aggressive behavior in mice. Proc. Natl. Acad. Sci. USA *108*, 12898–12903.
18. Oboti, L., Pérez-Gómez, A., Keller, M., Jacobi, E., Birnbaumer, L., Leinders-Zufall, T., Zufall, F., and Chamero, P. (2014). A wide range of pheromone-stimulated sexual and reproductive behaviors in female mice depend on G protein Gαo. BMC Biol. *12*, 31.
19. Pérez-Gómez, A., Stein, B., Leinders-Zufall, T., and Chamero, P. (2014). Signaling mechanisms and behavioral function of the mouse basal vomeronasal neuroepithelium. Front. Neuroanat. *8*, 135.
20. Chamero, P., Marton, T.F., Logan, D.W., Flanagan, K., Cruz, J.R., Saghatelian, A., Cravatt, B.F., and Stowers, L. (2007). Identification of protein pheromones that promote aggressive behaviour. Nature *450*, 899–902.
21. Leinders-Zufall, T., Ishii, T., Chamero, P., Hendrix, P., Oboti, L., Schmid, A., Kircher, S., Pyrski, M., Akiyoshi, S., Khan, M., *et al*. (2014). A family of nonclassical class I MHC genes contributes to ultrasensitive chemodetection by mouse vomeronasal sensory neurons. J. Neurosci. *34*, 5121–5133.
22. Schmid, A., Pyrski, M., Biel, M., Leinders-Zufall, T., and Zufall, F. (2010). Grueneberg ganglion neurons are finely tuned cold sensors. J. Neurosci. *30*, 7563–7568.
23. Leinders-Zufall, T., Cockerham, R.E., Michalakis, S., Biel, M., Garbers, D.L., Reed, R.R., Zufall, F., and Munger, S.D. (2007). Contribution of the receptor guanylyl cyclase GC-D to chemosensory function in the olfactory epithelium. Proc. Natl. Acad. Sci. USA *104*, 14507–14512.
24. Munger, S.D., Leinders-Zufall, T., McDougall, L.M., Cockerham, R.E., Schmid, A., Wandernoth, P., Wennemuth, G., Biel, M., Zufall, F., and

Kelliher, K.R. (2010). An olfactory subsystem that detects carbon disulfide and mediates food-related social learning. Curr. Biol. *20*, 1438–1444.

25. Zufall, F., and Munger, S.D. (2010). Receptor guanylyl cyclases in mammalian olfactory function. Mol. Cell. Biochem. *334*, 191–197.
26. Liu, C.Y., Fraser, S.E., and Koos, D.S. (2009). Grueneberg ganglion olfactory subsystem employs a cGMP signaling pathway. J. Comp. Neurol. *516*, 36–48.
27. Mamasuew, K., Hofmann, N., Kretzschmann, V., Biel, M., Yang, R.B., Breer, H., and Fleischer, J. (2011). Chemo- and thermosensory responsiveness of Grueneberg ganglion neurons relies on cyclic guanosine monophosphate signaling elements. Neurosignals *19*, 198–209.
28. Meyer, M.R., Angele, A., Kremmer, E., Kaupp, U.B., and Muller, F. (2000). A cGMP-signaling pathway in a subset of olfactory sensory neurons. Proc. Natl. Acad. Sci. USA *97*, 10595–10600.
29. Ma, M., Grosmaitre, X., Iwema, C.L., Baker, H., Greer, C.A., and Shepherd, G.M. (2003). Olfactory signal transduction in the mouse septal organ. J. Neurosci. *23*, 317–324.
30. Cockerham, R.E., Puche, A.C., and Munger, S.D. (2009). Heterogeneous sensory innervation and extensive intrabulbar connections of olfactory necklace glomeruli. PLoS ONE *4*, e4657.
31. Staples, L.G., McGregor, I.S., Apfelbach, R., and Hunt, G.E. (2008). Cat odor, but not trimethylthiazoline (fox odor), activates accessory olfactory and defense-related brain regions in rats. Neuroscience *151*, 937–947.
32. Johnson, M.A., Tsai, L., Roy, D.S., Valenzuela, D.H., Mosley, C., Magklara, A., Lomvardas, S., Liberles, S.D., and Barnea, G. (2012). Neurons expressing trace amine-associated receptors project to discrete glomeruli and constitute an olfactory subsystem. Proc. Natl. Acad. Sci. USA *109*, 13410–13415.
33. Pacifico, R., Dewan, A., Cawley, D., Guo, C., and Bozza, T. (2012). An olfactory subsystem that mediates high-sensitivity detection of volatile amines. Cell Rep. *2*, 76–88.
34. Fendt, M., Endres, T., Lowry, C.A., Apfelbach, R., and McGregor, I.S. (2005). TMT-induced autonomic and behavioral changes and the neural basis of its processing. Neurosci. Biobehav. Rev. *29*, 1145–1156.
35. Root, C.M., Denny, C.A., Hen, R., and Axel, R. (2014). The participation of cortical amygdala in innate, odour-driven behaviour. Nature *515*, 269–273.
36. Canteras, N.S. (2002). The medial hypothalamic defensive system: hodological organization and functional implications. Pharmacol. Biochem. Behav. *71*, 481–491.
37. Davis, M. (1992). The role of the amygdala in fear and anxiety. Annu. Rev. Neurosci. *15*, 353–375.
38. Li, C.I., Maglinao, T.L., and Takahashi, L.K. (2004). Medial amygdala modulation of predator odor-induced unconditioned fear in the rat. Behav. Neurosci. *118*, 324–332.
39. Dias, B.G., Banerjee, S.B., Goodman, J.V., and Ressler, K.J. (2013). Towards new approaches to disorders of fear and anxiety. Curr. Opin. Neurobiol. *23*, 346–352.
40. Canteras, N.S., Chiavegatto, S., Ribeiro do Valle, L.E., and Swanson, L.W. (1997). Severe reduction of rat defensive behavior to a predator by discrete hypothalamic chemical lesions. Brain Res. Bull. *44*, 297–305.
41. Motta, S.C., Goto, M., Gouveia, F.V., Baldo, M.V., Canteras, N.S., and Swanson, L.W. (2009). Dissecting the brain's fear system reveals the hypothalamus is critical for responding in subordinate conspecific intruders. Proc. Natl. Acad. Sci. USA *106*, 4870–4875.
42. Silva, B.A., Mattucci, C., Krzywkowski, P., Murana, E., Illarionova, A., Grinevich, V., Canteras, N.S., Ragozzino, D., and Gross, C.T. (2013). Independent hypothalamic circuits for social and predator fear. Nat. Neurosci. *16*, 1731–1733.
43. Lin, D., Boyle, M.P., Dollar, P., Lee, H., Lein, E.S., Perona, P., and Anderson, D.J. (2011). Functional identification of an aggression locus in the mouse hypothalamus. Nature *470*, 221–226.
44. Wheatley, M.D. (1944). Hypothalamus and affective behavior in cats: A study of the effects of experimental lesions, with anatomical correlations. Arch. Neurol. Psychiatry *52*, 296–316.
45. Lammers, J.H., Kruk, M.R., Meelis, W., and van der Poel, A.M. (1988). Hypothalamic substrates for brain stimulation-induced attack, teeth-chattering and social grooming in the rat. Brain Res. *449*, 311–327.
46. Freitas, R.L., Uribe-Mariño, A., Castiblanco-Urbina, M.A., Elias-Filho, D.H., and Coimbra, N.C. (2009). GABA($_A$) receptor blockade in dorsomedial and ventromedial nuclei of the hypothalamus evokes panic-like elaborated defensive behaviour followed by innate fear-induced antinociception. Brain Res. *1305*, 118–131.
47. Bueno, C.H., Zangrossi, H., Jr., and Viana, Mde.B. (2007). GABA/benzodiazepine receptors in the ventromedial hypothalamic nucleus regulate both anxiety and panic-related defensive responses in the elevated T-maze. Brain Res. Bull. *74*, 134–141.

 ©2015 Elsevier Ltd All rights reserved